J. Chem. Thermodynamics 48 (2012) 284–290

Contents lists available at SciVerse ScienceDirect

J. Chem. Thermodynamics

journal homepage: www.elsevier.com/locate/jct

High-pressure phase behaviour of the system (CO_2 + C.I. Disperse Orange 30 dye)

J.C. dos Santos [a], H.R. Mazzer [c], G.D. Machado [c], J. Andreaus [b], V.F. Cabral [c,*], M.S. Zabaloy [d], L. Cardozo-Filho [c]

[a] Departamento de Engenharia Têxtil, Universidade Estadual de Maringá, Av. Reitor Zeferino Vaz s/n, Goioerê, PR 87360-000, Brazil
[b] Departamento de Química, Universidade Regional de Blumenau, Rua Antônio da Veiga 140, Blumenal, SC 89012-900, Brazil
[c] Departamento de Engenharia Química, Universidade Estadual de Maringá, Av. Colombo 5790, Maringá, PR 87020-900, Brazil
[d] Departamento de Ingeniería Química, Universidad Nacional del Sur, Planta Piloto de Ingeniería Química, CONICET, Camino La Carrindanga Km 7, CC 717, (8000) Bahía Blanca, Argentina

ARTICLE INFO

Article history:
Received 8 July 2011
Received in revised form 22 November 2011
Accepted 30 December 2011
Available online 8 January 2012

Keywords:
Solid–fluid transition
Solubility
Textile dye
Peng–Robinson
High pressure
Carbon dioxide
SFD

ABSTRACT

The dyeing of textile fibres of poly-ethylene terephthalate (PET) in a supercritical medium is an environmentally friendly technological alternative to the conventional water-based dyeing process. In this work, the solubility of the monoazo disperse dye 4-((2,6-dichloro-4-nitrophenyl) azo)-N-(cyanoethyl)-N-(acetoxyethyl) aniline (CAS number 5621-31-4, also known as "C.I. Disperse Orange 30") in supercritical carbon dioxide (SC-CO_2) was experimentally studied within a dye mole fraction range from $6.55 \cdot 10^{-6}$ to $9.31 \cdot 10^{-6}$ and over the temperature range from (303.15 to 333.15) K. The resulting measured solid–fluid transition pressures fell in the range from (9.93 to 14.82) MPa. The measurements were performed using the static-synthetic method. The dye solubility in carbon dioxide was found to increase with increasing pressure. The experimental results were correlated with a model that combines the Peng–Robinson equation of state for describing the fluid phase and a standard equation for the fugacity of the pure dye in solid state. The reference state for such equation is the sublimation curve of the pure dye.

1. Introduction

The conventional industrial process for dyeing textile fibres uses water, both as the dyestuff solvent and as the solvent for the subsequent washings of the tissues. This leads to contaminated effluents that become major sources of pollution of the environment [1–5]. The contribution to pollution by these industries has therefore become a focus of research and monitoring for environmental care [25].

Some researchers have considered the use of supercritical fluid dyeing (SFD) (which does not require the use dispersing agents or surfactants) as an alternative to the conventional dyeing process. Such previous works reported convenient solubility values for various disperse dyes in supercritical carbon dioxide (SC-CO_2) [6–10], and also reported dyeing times lower than those of the conventional process [6].

Besides speeding up the production of the dyed fibres in the textile manufacturing process, the dyeing process with supercritical carbon dioxide requires a lower consumption of water [11]. It also minimizes the need for conventional auxiliary chemicals, as reported by some authors [18,19].

The knowledge of the phase behaviour of binary (supercritical solvent + dye) systems is required for the development of SFD processes. Of special importance is the study of the solubility in carbon dioxide of the dyes related to the dyeing process of filaments composed of poly-ethylene terephthalate (PET) or of other natural fibres [2,11–16].

To achieve an effective dyeing, the conventional industrial process for dyeing PET textile fibres is performed at high temperature, *e.g.*, at 403.15 K. This high temperature implies a high energy consumption which is substantially higher than that of the SFD process [20].

The experimental studies, available in the literature, on the solubility of solids of high molar mass in supercritical carbon dioxide, often do not cover the low solute concentration range (see, *e.g.*, [25]). The main purpose of the present study was to measure the solid–fluid transition pressure for the binary system (carbon dioxide + C.I. Disperse Orange 30) over the temperature range from (303.15 to 333.15) K, at dye mole fraction values below 10^{-5}, *i.e.*, in the low dye mole fraction range, which has not been covered in the literature [25].

Some empirical models have been used for describing the relationship between the density (or the pressure) of the supercritical solvent and the solubility of substances with high molar mass [25]. Cabral *et al.* [9] have proposed to correlate the dye solubility in a

* Corresponding author. Tel.: +55 44 3011 4749; fax: +55 44 3011 4792.
E-mail address: vladimir@deq.uem.br (V.F. Cabral).

0021-9614/$ - see front matter © 2012 Elsevier Ltd. All rights reserved.
doi:10.1016/j.jct.2011.12.040

way similar to that of Lee *et al.* [23,24]. Such approach [9], which combines the expanded liquid model with the Margules excess Gibbs energy model, does not require the critical properties of the dye as input information for performing the solubility calculations. Yamini *et al.* [20] correlated solubility data for a number of dyes in supercritical carbon dioxide using four semi empirical models (Chrastil, Kumar-Johnston, Bartle, and Mendez-Santiago-Teja). They [20] also estimated the enthalpies of dye–CO_2 solvation and dye vapourization. In the present work, the solubility of C.I. Disperse Orange 30 in pure SC-CO_2 was correlated with a model that couples a standard equation for the fugacity of the pure dye in solid state (solid phase) to the Peng–Robinson [29] (PR) equation of state (EOS) used with quadratic mixing rules (fluid phase). The reference state for the solid fugacity equation is the sublimation curve of the pure dye.

2. Experimental

2.1. Materials

The dyestuff C.I. Disperse Orange 30 (CAS number 5621-31-4, molar mass = 450.27 g · mol^{-1}), free from dispersing agents and surfactants, was supplied by Sinochem Jiangsu I/E Corp (Beijing, China). Its melting point was T_m = 398.75 K and its enthalpy of fusion was 31.85 kJ · mol^{-1}, both measured in this work by differential scanning calorimetry (Auto Q20 DSC, TA Instruments). The DSC equipment has an operating temperature range from (298.15 to 998.15) K and uses nitrogen as the coolant fluid. The coolant fluid flow rate was 50 dm^3 · min^{-1}. The volumetric method using helium gas was employed in the DSC measurements. The heating rate was 283 K · min^{-1}.

Carbon dioxide (min mass fraction purity 0.995) was supplied by Praxair Inc. and used without further purification. Figure 1 shows the molecular structure of C.I. Disperse Orange 30.

2.2. Experimental equipment and procedure

In view of the desired range of variation for the overall dye mole fraction, which has a calculated order of magnitude of 10^{-6}, the static synthetic method [21,22] was chosen in this work to carry out the phase transition measurements (figure 2).

The (solid + fluid) equilibrium apparatus was placed inside a bath equipped with a PID temperature controller (DIGI MEC mark, SHM 112 model). The controller was connected to a thermocouple (J type, with an uncertainty of 1.0 K), which was in direct contact with the fluid mixture inside the equilibrium cell. The thermocouple was calibrated using a primary thermometer (Incoterm, 47342 model) at four fixed temperatures ranging from (273 to 373) K. A temperature control within 1.0 K was achieved. The temperature was read in a temperature indicator (TI). The apparatus consists of a high-pressure variable-volume equilibrium cell (EC, 304 stainless steel) that has two sapphire windows: one (LW, diameter: 15.87 mm, thickness: 4.76 mm) for lighting the cell contents and the other for performing visual observations (OW, diameter: 25.4 mm, thickness: 9.52 mm). The EC has a maximum volume of 23 cm^3 and contains a piston (P), which makes possible to manipulate the pressure inside the cell. The hydraulic fluid in contact with the rear side of the piston is CO_2, which is forced to flow by the pressure control (syringe) pump (PP). The hydraulic fluid affects the position of the piston which in turn influences the pressure of the sample in contact with the front side of the piston. The pressure measurement and control is carried out with an absolute pressure transducer (Smar LD 301), with a precision of 0.01 MPa, a portable programmer (Smar, HT 201) for the pressure data acquisition, and a syringe pump (ISCO 260D). The pressure transducer was calibrated against a digital multimeter HP-34401A model.

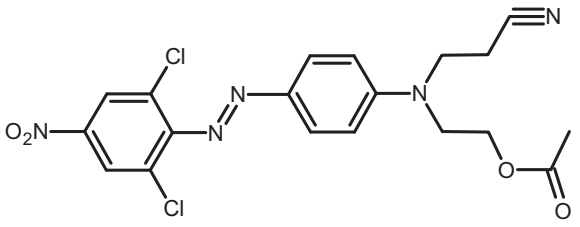

FIGURE 1. The molecular structure of C.I. Disperse Orange 30 dye.

The experimental procedure is as follows. First, a known mass of the dye (C.I. Disperse Orange 30) is loaded into the EC. Next, the air is removed from the system. Then, an amount of carbon dioxide, corresponding to the desired overall composition, is slowly injected (valve V5 opened) into the EC. The total amount of carbon dioxide introduced into the sample side of the cell is obtained from the measured volume of carbon dioxide in the PP before and after the CO_2 loading.

The cell content is kept under continuous agitation with the help of a Teflon-coated stirring bar, driven by a magnetic stirrer. After reaching the desired temperature, the sample pressure is increased by applying pressure on the back of the piston through the syringe pump, until a single phase is observed and maintained for at least 10 min. Next, the pressure is automatically decreased at a rate of 0.20 MPa · min^{-1}, until the formation of an incipient new phase is observed (solid–fluid transition). For a given temperature and overall composition, this procedure is repeated three times and the three observed transition pressures averaged. This leads to 0.01 MPa experimental standard deviations. The solid–fluid transition pressure is obtained as a function of temperature for each set overall composition, *i.e.*, a single loading of the EC is used for measuring the solid–fluid transitions over a range of pressure and temperature (isopleth, table 1).

It is clear that our procedure for measuring solid–fluid transitions consists of looking for the pressure of appearance of a solid phase, *i.e.*, we search for a freezing point rather than for a melting point. This was also the choice that Cheong *et al.* [30] made, on the grounds of a lower scattering of the data. Cheong *et al.* [30] ascribed the lower self-consistency of the melting point data, with respect to that of the freezing point data, to a possible non-uniformity of the fluid phase composition when the solid begins to melt.

In view of the validation performed in several previous works for the experimental apparatus and procedures used here, potential sub cooling effects associated to the search for the appearance of a new (solid) phase are considered to be non significant in the experimental results that we report in this work. Likewise, such validation experiments also indicate that the pressure gap through the cell piston is negligible.

As previously stated, in our experimental procedure we set the temperature and the overall composition of the system, and detect the pressure at which an incipient solid phase appears. The set made of the experimental temperature, the fluid composition and the experimental solid–fluid transition pressure is regarded, within the experimental uncertainty, as the phase equilibrium relationship among such variables. For this reason we refer to the concentration of the dye of a given experimental datum as the "solubility" of the dye in CO_2, at the experimental temperature and pressure. This is a standard practice, *i.e.*, the overall composition at which a solid–fluid transition experiment is carried out using to the synthetic method is named "solubility", as it has recently been done, *e.g.*, by Martín *et al.* [31]. Indeed, the "phase equilibrium" assumption is behind the use of the word "solubility".

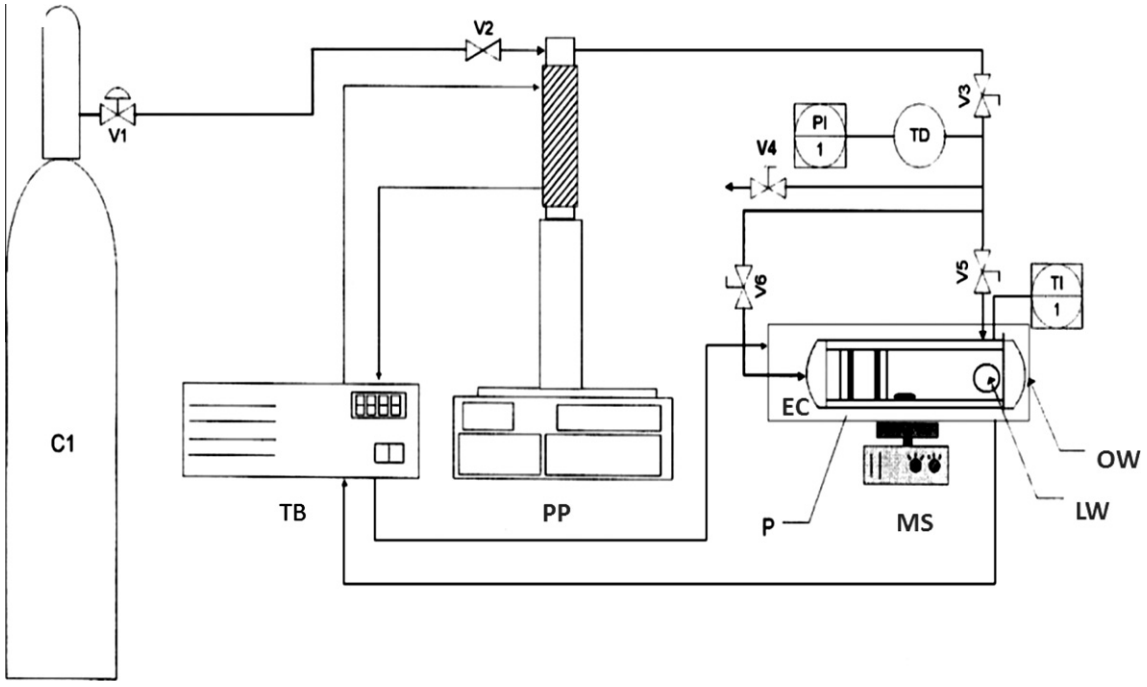

FIGURE 2. Schematic diagram of experimental apparatus: (c1) CO_2 cylinder; (V1, V2, V3, V4, V5 and V6) valves; (TD) pressure transducer; (PI/1) pressure indicator; (TI/1) temperature indicator; (OW) observation window; (LW) lighting window; (EC) equilibrium cell, stainless steel 23 cm^3 maximum capacity; (P) piston; (MS) magnetic stirrer; (PP) pressure control pump and (TB) thermostatic bath.

TABLE 1
Experimental Solid–Liquid Transition data for the system {CO_2 (1) + C.I. Disperse Orange 30 (2)}.

T/K	P/MPa	σ/MPa	ρ/g · cm^{-3}	Transition/Type
		$y_2 \cdot 10^6 = 6.55$		
303.15	11.20	0.01	0.7964	SF
313.15	10.78	0.01	0.6751	SF
323.15	10.44	0.01	0.4394	SF
333.15	9.93	0.01	0.2858	SF
		$y_2 \cdot 10^6 = 6.84$		
303.15	12.05	0.00	0.8104	SF
313.15	11.74	0.01	0.7111	SF
323.15	10.96	0.01	0.4999	SF
333.15	10.53	0.00	0.3245	SF
		$y_2 \cdot 10^6 = 7.00$		
303.15	12.55	0.01	0.8177	SF
313.15	12.11	0.01	0.7220	SF
323.15	11.68	0.01	0.5644	SF
333.15	11.37	0.01	0.3864	SF
		$y_2 \cdot 10^6 = 7.82$		
303.15	13.04	0.01	0.8245	SF
313.15	12.73	0.01	0.7379	SF
323.15	12.30	0.00	0.6041	SF
333.15	11.62	0.00	0.4059	SF
		$y_2 \cdot 10^6 = 8.58$		
303.15	13.56	0.00	0.8311	SF
313.15	13.26	0.01	0.7497	SF
323.15	12.73	0.01	0.6258	SF
333.15	12.14	0.001	0.4462	SF
		$y_2 \cdot 10^6 = 9.31$		
303.15	14.82	0.01	0.8457	SF
313.15	14.21	0.01	0.7680	SF
323.15	13.94	0.01	0.6717	SF
333.15	13.35	0.00	0.5283	SF

Estimated uncertainties u are $u(T) = 1.0$ K, $u(P) = 1.0$, $u(\rho) = 0.0001$.

3. Thermodynamic modelling

Due to the asymmetry of the system (carbon dioxide + C.I. Disperse Orange 30), it is assumed that under conditions of (solid + fluid) equilibrium the solid phase is made of the pure dye (component 2), whose fugacity f_2 is calculated as follows [27]:

$$f_2 = (P_2^{sat}/\text{bar}) \exp\left(\frac{(V_2^{sat}/\text{mL}\cdot\text{mol}^{-1})\,(P/\text{bar})}{R\,(T/\text{K})}\right), \tag{1}$$

where P_2^{sat} is the solid/vapour saturation pressure at temperature T and V_2^{sat} is the molar volume, both for the pure dye in solid state; P is the pressure of the system. The exponential factor in equation (1) is a Poynting correction. The fugacity ($\overline{f_2}$) of the dye in the fluid phase is given by the following equation [27]:

$$\overline{f_2} = y_2\,(P/\text{bar})\,\hat{\varphi}_2^{\infty}, \tag{2}$$

where $\hat{\varphi}_2^{\infty}$ is the fugacity coefficient of the dye at infinite dilution and y_2 is the mole fraction of the dye in fluid phase, *i.e.*, y_2 is the solubility of the dye in carbon dioxide. The condition of equilibrium, *i.e.*, the isofugacity condition, is the following:

$$\overline{f_2} = f_2, \tag{3}$$

which leads to the final equation used for computing the dye solubility y_2, *i.e.*, [27],

$$y_2 = \frac{(P_2^{sat}/\text{bar})}{(P/\text{bar})}\,\frac{1}{\hat{\varphi}_2^{\infty}}\,\exp\frac{(V_2^{sat}/\text{mL}\cdot\text{mol}^{-1})(P/\text{bar})}{R\,(T/\text{K})}. \tag{4}$$

The use of equation (4) requires the knowledge of P_2^{sat} and V_2^{sat}. Besides, the fugacity coefficient $\hat{\varphi}_2^{\infty}$ is calculated in this work using the Peng–Robinson [29] equation of state (PR-EOS) with classical quadratic mixing rules. The expressions of the PR-EOS and mixing rules are the following:

$$\frac{P}{\text{bar}} = \frac{R\,(T/\text{K})}{v-b} - \frac{a}{v(v+b)+b(v-b)}, \tag{5}$$

$$a = \sum_{i=1}^{nc}\sum_{j=1}^{nc} y_i y_j \sqrt{a_i a_j}(1-k_{ij}), \tag{6}$$

TABLE 2
Critical properties (T_c and P_c) and acentric factors (ω) of CO_2 and "C.I. Disperse Orange 30" used in the thermodynamic modelling.

Dye	T_C/K	P_C/MPa	ω
CO_2*	304.2	7.383	0.224
C.I. Disperse Orange 30	1370.5	1.45	1.339

* The values of critical properties and acentric factor of CO_2 were taken from reference [27].

TABLE 3
Interaction parameters k_{ij}, l_{ij} and sublimation pressure P_2^{sat} for the system {CO_2 (1) + C.I. Disperse Orange 30 (2)}.

T/K	Parameters			
	k_{ij}	l_{ij}	P_2^{sat}/MPa	AAD%
303.15	0.6915	0.6046	$5.28 \cdot 10^{-11}$	3.12
313.15	0.7694	0.6456	$2.16 \cdot 10^{-8}$	4.77
323.15	0.7381	0.5183	$8.78 \cdot 10^{-8}$	6.98
333.15	0.7729	0.5191	$8.69 \cdot 10^{-7}$	6.28

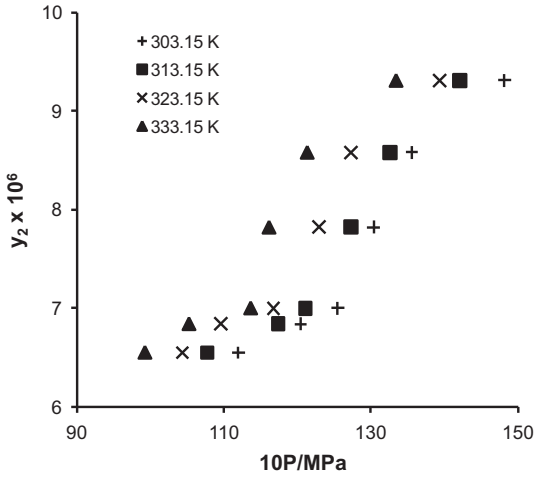

FIGURE 3. Solubility of C.I. Disperse Orange 30 in SC-CO_2 (y_2) as a function of pressure, in a temperature range. Markers: experimental (solid + fluid) equilibrium data obtained in this work.

$$b = \sum_{i=1}^{nc}\sum_{j=1}^{nc} y_i y_j \left(\frac{b_i + b_j}{2}\right)(1 - l_{ij}), \tag{7}$$

where y_i is the mole fraction of component i, k_{ij} and l_{ij} are the binary interaction parameters, and v is the fluid phase molar volume. The pure component parameters a_i and b_i are given by the following equations:

$$a_i = \left(\frac{0.4572\, R^2 (T_{c_i}/\mathrm{K})^2}{(P_{c_i}/\mathrm{bar})}\right)\Big[1 + (0.37464 + 1.5422\omega_i - 0.26992\omega_i^2)(1 - \sqrt{T_{r_i}})\Big]^2, \tag{8}$$

$$b_i = 0.07780\, R \frac{(T_c/\mathrm{K})}{(P_c/\mathrm{bar})}, \tag{9}$$

where T_{c_i}, P_{c_i}, ω_i and $T_{r_i}(= T/T_{c_i})$ are the critical temperature, critical pressure, acentric factor, and reduced temperature of component "i", respectively. The values of the critical properties and acentric factor of the dye were calculated using the group contribution method of Joback [26]. Their values are reported in table 2.

The value of 273 $dm^3 \cdot mol^{-1}$ was used for the molar volume of the solid, V_2^{sat} [25]. The parameters k_{ij}, l_{ij}, and P_2^{sat} were fit by matching equation (4) to the solubility experimental data obtained in this work. The final parameter values are reported in table 3, which also presents the average absolute-value percent deviation (AAD%) for each isotherm.

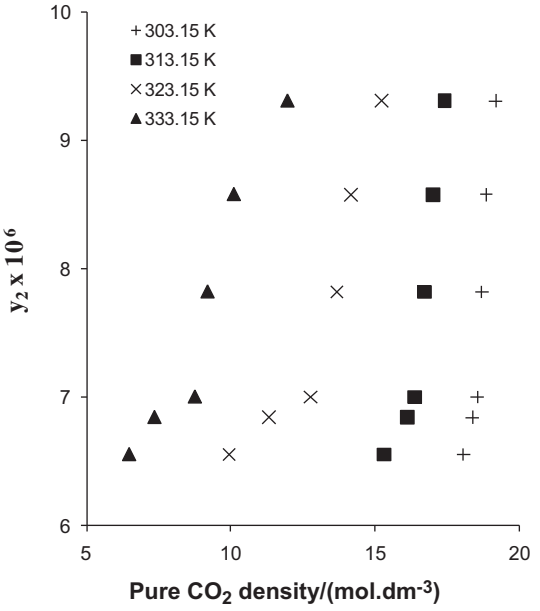

FIGURE 4. Solubility of C.I. Disperse Orange 30 in SC-CO_2 (y_2) as a function of pure SC-CO_2 density, for the temperature range shown. Markers: experimental (solid + - fluid) equilibrium data obtained in this work.

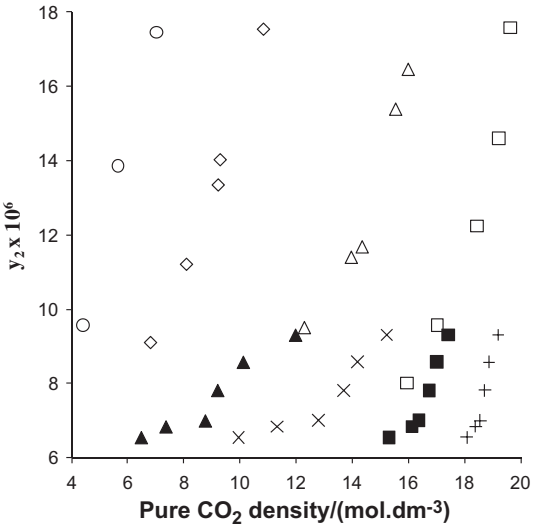

FIGURE 5. Solubility of C.I. Disperse Orange 30 in SC-CO_2 (y_2) as a function of pure SC-CO_2 density, in a temperature range. Comparison between the experimental (solid + fluid) equilibrium data obtained in this work and those obtained by Baek *et al.* [25]. Symbols: +: T = 303.15 K (this work); filled squares: 313.15 K (this work); empty squares: 313.15 K [25]; ×: 323.15 K (this work); filled triangles: 333.15 K (this work); empty triangles: 333.15 K [25]; empty rhombuses: 363.15 K [25]; empty circles: 393.15 K [25].

This AAD% parameter is defined by the following equation:

$$\mathrm{AAD}\% = \frac{1}{np}\sum_{i=1}^{np}\left(\frac{|y_{2_i}^{\mathrm{exp}} - y_{2_i}^{\mathrm{calc}}|}{y_{2_i}^{\mathrm{exp}}}\right) \times 100, \tag{10}$$

where np is the number of experimental data points, and $y_{2_i}^{\mathrm{exp}}$ and $y_{2_i}^{\mathrm{calc}}$ are the experimental and calculated dye solubilities, respectively.

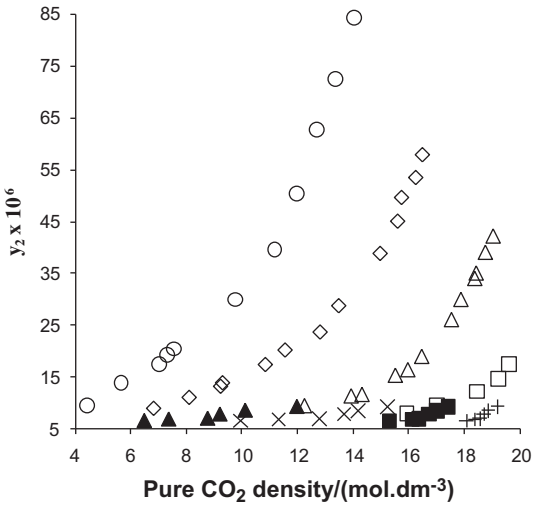

FIGURE 6. Solubility of C.I. Disperse Orange 30 in SC-CO_2 (y_2) as a function of pure SC-CO_2 density, in a temperature range. Comparison, in a pressure range wider than that of figure 5, between the experimental (solid + fluid) equilibrium data obtained in this work and those obtained by Baek *et al.* [25]. Symbols: +: T = 303.15 K (this work); filled squares: 313.15 K (this work); empty squares: 313.15 K [25]; ×: 323.15 K (this work); filled triangles: 333.15 K (this work); empty triangles: 333.15 K [25]; empty rhombuses: 363.15 K [25]; empty circles: 393.15 K [25].

4. Results and discussion

4.1. Experimental results

The experimental solid–fluid transition data obtained in this work for the system {CO_2 (1) + C.I. Disperse Orange 30 (2)} are reported in table 1. The dye mole fraction range is $6.55 \cdot 10^{-6}$ to $9.31 \cdot 10^{-6}$, and the temperature range is (303.15 to 333.15) K. The measured solid–fluid transition pressures fall in the range (9.93 to 14.82) MPa. The pure CO2 density values for every experimental data point in table 1 were calculated using the NIST web site [28]. Figure 3 presents the dye solubility as a function of pressure at four different temperature values. For a given data point at a pressure greater than the experimental pressure, the system is made of an homogeneous fluid phase, while at a pressure less than the experimental pressure the system is heterogeneous, *i.e.*, made of a fluid phase and of a solid phase.

Figure 3 shows that at constant dye solubility the pressure decreases with increasing temperature. Following Baek *et al.* [25], we present in figure 4 the solubility of C.I. Disperse Orange 30 in SC-CO_2 (experimental data obtained in this work) as a function of the density {NIST, [28]} of pure SC-CO_2, in a temperature range.

The information shown in figure 4 is also presented in figure 5, where the data obtained by Baek *et al.* [25] at low enough pressure are also displayed. The filled and empty triangles are, respectively, our data and those of Baek at T = 333.15 K: both data sets appear to fall on a single curve. This is indicative of good agreement. At T = 313.15 K our data (filled squares) correspond to values of solubility slightly lower than those of Baek *et al.* [25] (empty squares). This is less important than it looks, since error bars were not drawn in figure 5. Finally, our data at T = 303.15 K (+) and at T = 323.15 K (×) are consistent with the temperature dependence of all the other data in figure 5. From figure 5, we therefore conclude that there is a good degree of agreement between the data by Baek *et al.* [25] and the experimental results obtained in this work.

Figure 6 presents again all our data and, this time, all the data of Baek *et al.* [25], which cover a pressure range from (11 to 33) MPa [25]. The reason for plotting our data together with data from the

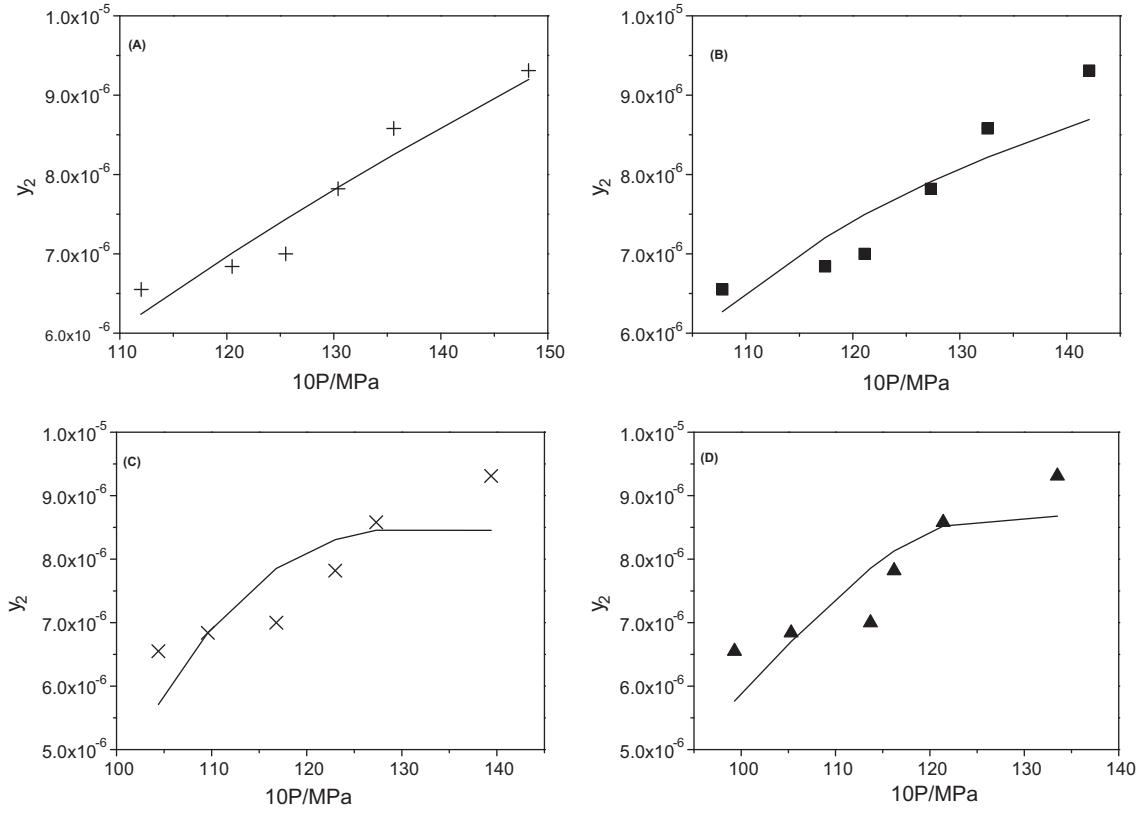

FIGURE 7. Solubility (y_2) of the C.I. Disperse Orange 30 (2) in CO_2 (1) as a function of the pressure for varying temperatures: (A) 303.15 K, (B) 313.15 K, (C) 323.15 K, (D) 333.15 K: Experimental data (this work) – PR-EOS coupled to equation (4).

literature on the solubility–density plane, rather than on the solubility-pressure plane, is that the isotherms may cross each other in the solubility-pressure plane [25]. This does not happen in the solubility–density plane [25].

Draper *et al.* [17] have also obtained experimental data on the solubility of C.I. Disperse Orange 30 in carbon dioxide. However, the melting point for this dye, declared by Draper *et al.* [17], is T_m = 382 K, which does not compare well with the melting point of the C.I. Disperse Orange 30 used in this work, *i.e.*, T_m = 398.75 K (see section 2.1). Similarly, while we have measured in this work an enthalpy of fusion of 31.85 kJ · mol^{-1} for the pure dye, Draper *et al.* [17] reported a value of 91.65 kJ · mol^{-1}, *i.e.*, roughly 190% higher than our value. Besides, Draper *et al.* [17] have not specified whether their C.I. Disperse Orange 30 was available in te pure state or in commercial form with dispersing agents and diluents present. They [17] have not identified the suppliers of the dye either. For these reasons, we do not present comparisons between our data and those of Draper *et al.* [17]. It is worth noting that the C.I. Disperse Orange 30 used by Baek *et al.* [25] had melting point of T_m = 398.56 K which compares extremely well with the value measured in the present work, *i.e.*, 398.75 K. On the other hand, Baek *et al.* [25] measured an enthalpy of fusion for the dye of 17.08 kJ · mol^{-1} which is lower than the heat of fusion measured in the present work, *i.e.*, 31.85 kJ · mol^{-1}. In spite of this difference, it is clear that our heat of fusion value (31.85 kJ · mol^{-1}) is much closer to the one by Baek *et al.* [25] (17.08 kJ · mol^{-1}) than to the one by Draper *et al.* [17] (91.65 kJ · mol^{-1}). Finally, Baek *et al.* [25] did declare that their C.I. Disperse Orange 30 dye was pure and contained neither dispersing agents nor surfactants, as it is the case for the dye used in this work. All these reasons make the comparison carried out in figure 5 meaningful.

4.2. Correlation results

Figure 7 presents the results for the correlation of the solubility of C.I. Disperse Orange 30 obtained using equation (4) coupled to the PR-EOS, for all the temperature values of our experiments, *i.e.*, from T = (303.15 to 333.15) K. The AAD% has values between 3% and 7% (table 3).

We observe that equation (4), coupled to the PR-EOS used with classical quadratic mixing rules, provides, at the parameter values of table 3, a fair agreement between the experimental and the calculated solubility values: the calculated solubility curves have a curvature opposite to that of the experimental data. The logarithm of the solid/vapour pure dye saturation pressure is known to decrease with the inverse temperature, *i.e.*, this property can be represented by the Clausius/Clapeyron equation. To verify this dependence and validate our estimation, the ln P^{sat} was plotted as a function of inverse temperature. Figure 8 shows the linear fit of the pure dye solid–vapour saturation pressures that we previouly obtained from regressing binary solubility data (table 3).

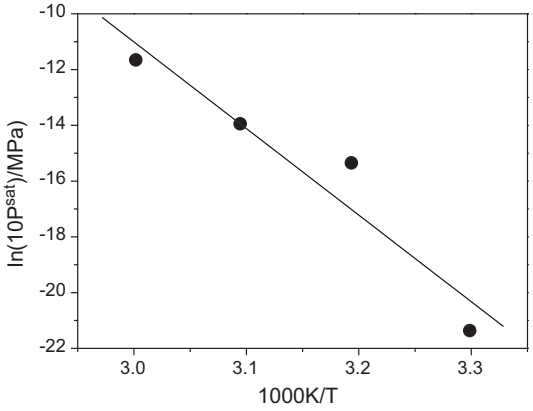

FIGURE 8. Temperature dependency of the pure dye solid/vapour saturation pressure. ■: Saturation pressure data regressed from the binary CO_2-dye solubility data of this work (see values in table 3) – Clausius/Clapeyron equation. The dye is C.I. Disperse Orange 30.

5. Remarks and conclusions

In this work we measured the solubility of "C.I. Disperse Orange 30" in supercritical carbon dioxide in the low dye concentration range, *i.e.*, the dye mole fraction of the experiments ranged from $6.55 \cdot 10^{-6}$ to $9.31 \cdot 10^{-6}$. The temperature and pressure ranges of the experiments were (303.15, 333.15) K and (9.93, 14.82) MPa, respectively. At constant temperature, the solubility of the dye in CO_2 increases with pressure. On the other hand, a temperature increase at constant dye concentration reduces the solid–fluid transition pressure. The experimental data obtained in this work extend the data of Baek *et al.* [25] to lower dye concentrations. The present data are consistent with the data of Baek.

The Peng–Robinson equation of state used with classical quadratic mixing rules, and combined with a standard pure solid dye fugacity equation, which uses the sublimation curve as reference state, was found to fairly correlate the solubility data within the ranges of conditions of the conducted experiments. The final parameter values do not give the right curvature of the solubility isotherms.

The results of this work are useful for studying the dyeing of PET in supercritical medium, which, due to the significantly lower dyeing temperature, requires a significantly lower energy consumption than the conventional process.

References

[1] J. Fasihi, Y. Yamini, F. Nourmohammadian, N. Bahramifar, Dyes and Pigments 63 (2004) 161–168.
[2] P. Dong, M. Xu, X. Lu, C. Lin, Fluid Phase Equilibr. 297 (2010) 46–51.
[3] A. Hou, B. Chen, J. Dai, K. Zhang, J. Cleaner Prod. 18 (2010) 1009–1014.
[4] K. Mishima, K. Matsuyama, H. Ishikawa, K. Hayashi, S. Maeda, Fluid Phase Equilibr. 194 (2002) 895–904.
[5] M.D. Gordillo, C. Pereyra, E.J. Martínez de la Ossa, Dyes and Pigments 67 (2005) 167–173.
[6] K.-H. Chang, H.-K. Bae, J.-J. ShinShim, Korean J. Chem. Eng. 13 (3) (1996) 310–316.
[7] W.L.F. Santos, R. Favareto, V.F. Cabral, E. Muniz, C. Cardozo-Filho, A.F. Rubira, J. Supercrit. Fluids 38 (2006) 319–325.
[8] H. Lin, C. Liu, C. Cheng, Y. Chen, M. Lee, J. Supercrit. Fluids 21 (2001) 1–9.
[9] V.F. Cabral, W.L.F. Santos, E.C. Muniz, A.F. Rubira, L. Cardozo-Filho, J. Supercrit. Fluids 40 (2007) 163–169.
[10] W. Saus, D. Knittel, E. Schollmeyer, Textile Res. J. 63 (1993) 135–142.
[11] Z.T. Liu, L. Zhang, Z. Gao, W. Dong, H. Xiong, Y. Peng, S. Tang, Ind. Eng. Chem. Res. 45 (2006) 8932–8938.
[12] H.K. Bae, J.W. Lee, W.P. Min, Fluids Phase Equilibr. 173 (2000) 277–284.
[13] A. Schimidt, E. Bach, E. Schollmeyer, Dyes and Pigments 56 (2003) 27–35.
[14] M. Banchero, A. Ferri, L. Manna, J. Supercrit. Fluids 48 (2009) 72–78.
[15] A. Ferri, M. Banchero, L. Manna, S. Sicardi, J. Supercrit. Fluids 30 (2004) 41–49.
[16] T. Shinoda, K. Tamura, Fluid Phase Equilibr. 213 (2003) 115–123.
[17] S.L. Draper, G.A. Montero, B. Smith, K. Beck, Dyes and Pigments 45 (2000) 177–183.
[18] M. van der Kraan, M.V. Fernandez Cid, G.F. Woerlee, W.J.T. Veugelers, G.J. Witkamp, J. Supercrit. Fluids 40 (2007) 470–476.
[19] P.S. Vankar, R. Shanker, A. Verma, J. Cleaner Prod. 15 (2007) 1441–1450.
[20] Y. Yamini, M. Moradi, M. Hojjati, F. Nourmohammadian, A. Saleh, J. Chem. Eng. Data 55 (2010) 3896–3900.
[21] M.L. Corazza, L. Cardozo-Filho, O.A.C. Antunes, C. Dariva, J. Chem. Eng. Data 48 (2003) 354.
[22] M.A. McHugh, V.J. Krukonis, Supercritical Fluid Extraction: Principles and Practice, Butterworth-Heinemann, London, 1994.
[23] J.W. Lee, J.M. Min, H.K. Bae, J. Chem. Eng. Data 44 (1999) 684–687.
[24] J.W. Lee, M.W. Park, H.K. Bae, Fluid Phase Equilibr. 173 (2000) 277–284.
[25] J.K. Baek, S. Kim, G.-S. Lee, J.J. Shim, J. Korean Chem. Eng. 21 (2004) 230–235.
[26] B.E. Poling, J.M. Prausnitz, J.P. ÓConnell, The Properties of Gases & Liquids, fifth ed., McGraw-Hill, New York, 2000.

[27] J.M. Smith, H.C. Van Ness, M.M. Abbot, Introduction to Chemical Engineering Thermodynamics, seventh ed., McGraw-Hill, New York, 2005.
[28] E.W. Lemmon, M.O. McLinden, D.G. Friend, "Thermophysical Properties of Fluid Systems" in NIST Chemistry WebBook, NIST Standard Reference Database Number 69, in: P.J. Linstrom, W.G. Mallard (Eds.), National Institute of Standards and Technology, Gaithersburg MD, 20899, http://www.webbook.nist.gov, (retrieved May 5, 2011).
[29] D.-Y. Peng, D.B. Robinson, Ind. Eng. Chem. Fundam. 15 (1976) 59–64.
[30] P.L. Cheong, D. Zhang, K. Ohgaki, B.C.-Y. Lu, Fluid Phase Equilibr. 29 (1986) 555–562.
[31] A. Martín, S. Rodríguez-Rojo, L. de Pablo, M.J. Cocero, J. Chem. Eng. Data 56 (2011) 3910–3913.

JCT-11-290